Sensors and Actuators: A. Physical 332 (2021) 113115

Contents lists available at ScienceDirect

Sensors and Actuators: A. Physical

journal homepage: www.elsevier.com/locate/sna

An untethered mechanically-intelligent inchworm robot powered by a shape memory alloy oscillator

Sean Thomas, Paolo Germano, Thomas Martinez, Yves Perriard*

Integrated Actuators Laboratory, Ecole Polytechnique Fédérale de Lausanne (EPFL), Switzerland

ARTICLE INFO

Article history:
Received 4 August 2021
Received in revised form 13 September 2021
Accepted 14 September 2021
Available online 6 October 2021

Keywords:
Smart material
Artificial muscle
Bio-inspired
Self-biasing
Compliant mechanism
Thermal model
Analytical model

ABSTRACT

Shape Memory Alloy (SMA) based actuators have become ideal candidates for use in compact and lightweight applications. These smart materials have often been referred to as artificial muscles due to their high work volume density. In this paper, a flexure-based SMA powered mechanical oscillator is developed to create an inchworm robot. Here, a novel magnetic latch system is used to create a mechanically-intelligent system that allows the abstraction of any sensors such as temperature probes. This insect robot, weighing only 9.7 g, operates without any control logic or micro-controller and is able to perform a crawling gait untethered. An analytical model of the thermal properties of the SMA coil, for the sizing of the robot speed, and an analytical model of the step length of the insect robot is presented and validated. A working prototype, with a speed of 1.55 mms^{-1}, is showcased in this work.

1. Introduction

Shape Memory Alloys (SMAs), often referred to as artificial muscles, are a type of smart material that is considered to have the highest volumetric work density [1,2]. These thermally activated materials are often used in lightweight and compact applications that still require high forces [3]. These alloys are able to recover any strain experienced at lower temperatures when they are heating above their transition temperature. Thus, they are often paired with a biasing element such as a spring, to create a lightweight reversible linear actuator.

A linear actuator, which can realize linear strokes without any transducer or conversion mechanisms to transform a rotational motion, can increase the efficiency and fatigue life. As mentioned earlier, only by pairing the SMA with a biasing element such as a passive spring, a basic linear actuator can be created [4]. By alternating between heating and cooling the SMA, a mechanical oscillator can be created [5]. However, due to the complex nature of the Shape Memory Effect (SME), complex control strategies are required to control the temperature and position of the SMA actuator [6–8]. These linear oscillators, which have flourished rapidly due to advances in materials and control technologies, can be used in applications such as compressors, pumps or, as showcased in this work, as insect-inspired crawling robots [9].

Recently, SMA powered linear actuators have grown in popularity creating these bio-inspired mobile robots that are able to mimic the gait of various mesoscale insects [10]. In particular, the rhythmic nature of SMA linear oscillators has made it the ideal candidate to create a crawling robot that mimics the locomotion of the inchworm. These inchworms are able to move forward by periodically activating their abdominal muscles [11].

These SMA driven crawling robots are generally quite large and wastes the high work density of the SMA due to the requirement of large biasing-springs and control electronics [12]. Furthermore, when designing these small scale robots, to reduce the weight, the SMAs are driven in an open loop with a risk of overheating and destroying the active material [13]. In this work, a mechanically intelligent, electronics-free control strategy will be presented to create the SMA actuated mechanical oscillator that powers this lightweight crawling robot. This removes the need for any micro-controller or sensors to be integrated into the robot design as opposed to most SMA inchworm solutions [14]. Here, *NiTiNOL*, a commonly used and readily available type of thermally activated SMA is used as the artificial muscle. Furthermore, the bias-spring, presented in this work, will use the inherent stiffness of the flexure-based mechanisms required for the implementation of the insect

* Correspondence to: Integrated Actuators Laboratory, Ecole Polytechnique Fédérale de Lausanne (EPFL), Neuchâtel 2000, Switzerland.
E-mail address: yves.perriard@epfl.ch (Y. Perriard).

https://doi.org/10.1016/j.sna.2021.113115
0924-4247/

robot. This results in a more compact and lightweight solution compared to the traditional bias-spring SMA actuator.

The paper is organized as follows: In Section 2, a gait analysis of the inchworm and the working principle of an SMA actuator will be presented. In Section 3, the working principle and a mechanically-intelligent control system for the SMA oscillator will be demonstrated, along with a thermal model for the SMA coil. In Section 4, the inchworm robot will be showcased along with an analytical model for its step length and locomotion. Lastly, in Section 5, the results of the crawling robot are examined, along with the validation of the analytical models. Finally, the future perspectives of such a design strategy are discussed with the possible limitations of this implementation.

2. Background

2.1. Biological analysis

The mobile robot presented in this work is inspired by the gait of the inchworm. The inchworm is not a type of worm but a type of caterpillar. These insects have a peculiar type of locomotion made possible by a looping motion called the two-anchor crawling gait [15]. Its gait consists of anchoring its forelegs and using the muscles present in its mid-section to pull the rest of its body as shown in Fig. 1.

The locomotion, as seen in Fig. 1, consists of alternating between gripping the ground or slipping. First, the forelegs are made to slip and the abdominal muscles are used to push against the hind legs to extend the forelegs. Next, the forelegs grip the ground and the abdominal muscles pull the hind legs which now slip against the ground. This pattern repeats to allow the inchworm to crawl along the surface. In this paper, artificial muscles, using smart materials, are used to replicate the gait of the inchworm.

2.2. Shape memory effect

Shape Memory Alloys (SMA) are a common type of artificial muscles that react mechanically to heat. This smart material exhibits the Shape Memory Effect (SME) based on phase transformations induced by temperature and stress. At room temperature, the material when exerted to a certain stress deforms *plastically*. This deformation can then be reversed and forced to return to its original shape by heating the material above its transition temperature. This behaviour can be exploited by pairing the alloy with a biasing element such as a dead weight or a spring to create a lightweight artificial muscle.

2.3. Bias-spring actuator

Often, the simplest solution for creating the actuator is to pair an SMA coil with a bias-spring. As seen in Fig. 2, the spring can be stretched by the SMA coil at high temperature while at low

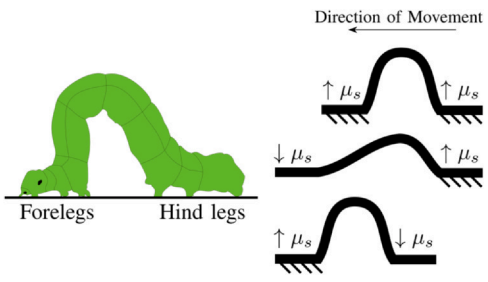

Fig. 1. The gait analysis of an inchworm showing the insect change the coefficient of friction (μ_s) with respect to the ground by either gripping or sliding its legs.

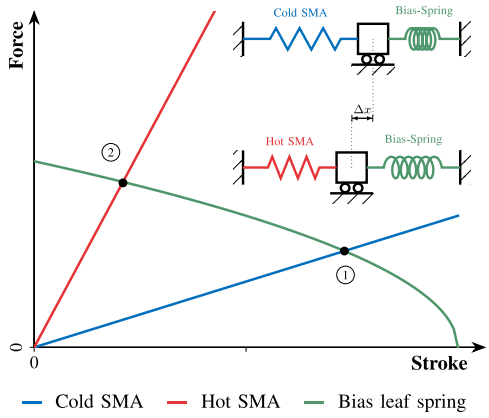

Fig. 2. A basic force-displacement graph to show the working principle of a bias-spring (in this case, a flexure-based spring) SMA linear actuator.

temperature, the SMA coil is stretched instead by the spring. The positions, shown in the figure as ① and ②, represent the stroke of the bias-spring actuator as the temperature of the SMA is alternated between hot and cold, respectively.

Increasing the stroke of the actuator requires increasing the length of the spring and the SMA. But this runs the risk of unwanted buckling and thus, often requiring the need for a linear guide for the actuator. In this work, the traditional bias-spring SMA actuator is adapted to used flexure-based linear guides rather than the traditional linear ball bearing kind consisting of rails. Usually, flexure-based mechanisms present with an unwanted inherent stiffness which is a drawback in most applications. But in this case, this inherent stiffness can be exploited to replace the biasing element. The linear stage flexure mechanism, as shown in Fig. 4, is composed of two parallel leaf springs which allow movement along one axis and inhibit the degrees of freedom is the other two axes. This strategy results in an improved work weight density for the actuator and a more compact solution that requires fewer parts as the biasing system and linear guides are combined. In this work, the flexural mechanism is 3D printed using PLA plastic and the stiffness of the spring can be calculated using the work in [16].

3. Mechanically-intelligent oscillator

With the traditional bias-spring SMA actuator, a simple back and forth oscillating motion can be created by heating and cooling the active material [4]. This kind of oscillator would require an accurate control of the temperature of the SMA. Since, the SME is a complex and highly non-linear behaviour, such control would require a sensor, such as a temperature sensor or position sensor, to establish a closed-loop control for accurate frequency control [6–8].

In this section, a sensor-less, electronics-free proof of concept is presented. The basic concept of this methodology is to tie the mechanical behaviour of the actuator into the control. The SMA retracts when a current is passed through due to Joule's losses. This retraction is used to mechanically cut the current flow across the SMA and allow the thermal exchange with air to cool down the SMA once again. The extension, upon cooling, is used to re-establish the electrical contact across the SMA, restarting the oscillating motion. Thus, this system allows an automatic oscillation of the bias-spring SMA actuator without any external sensor or control electronics [5].

3.1. Implementation

As mentioned earlier, using a flexure based mechanism as a linear guide, permits the omission of a dedicated spring in the design. As seen in Fig. 4, the linear stage is comprised of a cantilever

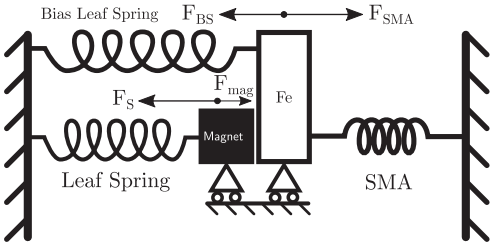

Fig. 3. Diagram showing the working principle of the SMA oscillator using the magnetic latch system.

beam. This cantilever act as a leaf spring that applies a tractional return force on the SMA coil at a lower temperature while also preventing any unwanted degrees of freedom in the other axis.

The implementation of the oscillator mechanism consists of pairing the SMA actuator with a magnetic latch system. A diagram of the working principle of the prototype can be seen in Fig. 3. The magnetic latch consists of a magnet mounted on a leaf spring that is attracted to the free end of the SMA actuator. The electrical current is made to flow across the magnetic latch and into the SMA coil. Thus, the coil is only heated when the magnet makes contact with the free end of the actuator. Essentially, as the magnet connects to the actuator, the coil is heated and retracts. As the coil retracts, the magnet mounted on the leaf spring is displaced with the coil. During this phase, the magnet experiences a return force, F_S, and will continue to follow the actuator. Once, the return force is higher than the attractive magnetic force, F_{mag}, between the magnet and the SMA coil, the latch detaches immediately from the actuator and the magnet returns to its original location. This causes the electrical contact to be broken and begins the cooling of the SMA coil. The bias leaf spring of the SMA actuator will, in this phase, extend the coil back towards the magnetic latch to, once again, re-establish the electrical contact. In this manner, an oscillating behaviour can be observed without any control logic or sensors. Therefore, the required contraction of the SMA coil, ε, can be controlled by sizing the leaf spring associated with the magnet.

$$\varepsilon = \frac{F_{\text{mag}}}{K_s} \tag{1}$$

where K_s is the rigidity of the leaf spring which depends on the dimensions of the cantilever beams and can be calculated using [16,17].

This basic concept can be implemented using different methods. The linear stages can be further optimised and sized to fit the desired stroke of the actuator. Solutions involving bistable mechanical latches and pogo pins can be imagined to serve the same purpose.Fig. 4.

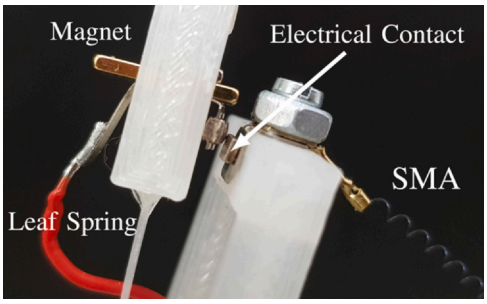

Fig. 4. The closeup of the magnetic latch system that acts as the oscillating electrical contact for the SMA coil. Here, electrical contacts from relays are used to reduce the resistance and an air gap is used to control the magnetic force.

3.2. Sizing of the oscillator

The SME is a thermomechanical behaviour and thus, the sizing of the oscillator is dependant on the temperature of the SMA coil as heating is generated by Joule's losses over the SMA. The rise time of the oscillator is directly related to the amplitude of the current applied across the SMA while the fall time of the oscillator is dictated by the cooling time of the SMA coil. In this case, the cooling occurs passively through thermal exchange with the surrounding air. Thus, the cooling time is related to the geometry of the SMA coil.

The amplitude of the oscillator is represented by the stroke of the bias-spring SMA actuator and as seen in the Fig. 2 depends on the stiffness of the bias-spring and the force-deformation curve of the SMA element. This stroke can be calculated using the analytical model of the SMA and the stiffness model of the spring as shown in [18] based on the Brinson model [19].

The cooling time of the SMA can be calculated using a simple thermal model based on the loss of thermal energy from the surface of the SMA wire and the surrounding air. The time constant, τ, of such a system can be expressed as:

$$\tau = \rho c d / (kH) \tag{2}$$

where ρ [kgm^{-3}] is the density, c [Jkg^{-1}K^{-1})] is the specific heat capacity, d is the wire diameter, $k = 4$ is the ratio between the surface area of heat exchange, A_S, and the volume of the active element, V, and H [Wm^{-2}K^{-1}] is the heat transfer coefficient. The thermal model of the wire can be expressed as:

$$T(t) = T_R + (T_2 - T_R)e^{-t/\tau} \tag{3}$$

where T_R is the ambient room temperature and t is time. Thus, the cooling time, t_c, based on the temperature gradient between the SMA and the surrounding air, can be expressed as:

$$t_c = \tau \log \frac{T_2 - T_R + \frac{T_2 - T_1}{2}}{T_2 - T_R - \frac{T_2 - T_1}{2}} \tag{4}$$

where the subscripts, 1 and 2, represents the operating points of the actuator as shown in Fig. 2. The physical properties of the SMA were obtained by consulting the data given by the supplier at *Dynalloy*.

Using equation 3, least-squares minimization is used to fit this thermal model to the cooling time of an SMA coil of 250 μm wire diameter. By doing so, the heat transfer coefficient, H, can be estimated. Using the model and the estimated parameters, the time constant and cooling times of other diameter SMA springs can be extrapolated. In Fig. 5, the cooling based on wire diameter of different SMA springs can be seen. This model is validated using a 200 μm diameter SMA coil which is then used in the proposed inchworm. Using these values, the fall time of the oscillator can be estimated for other wire diameters.

The rise time of the oscillator, t_h, can be estimated by calculating the time required to heat the SMA wire using Joule heating. Using the known resistance of the SMA wire, R, and the current, I, supplied to the system the heating time can be easily measured using the basic laws of electro-thermodynamics. In the case of slower rise time with small currents, the loss of heat with the surrounding air by convection must be taken into account and can be estimated with the equation:

$$t_h = \int_{T_1}^{T_2} \frac{\rho V c}{I^2 R(T) - H A_S (T - T_R)} dT \tag{5}$$

The repeatability of the system has been presented in the previous work [20] and has shown that when the oscillator has been left to oscillate, its frequency has remained consistent. However, when considering the actuator, the life cycle of the SMA coil depends greatly on the strain amplitude and the type of imposed stress. Based on work in the field [21] and considering that the SMA coil is under a

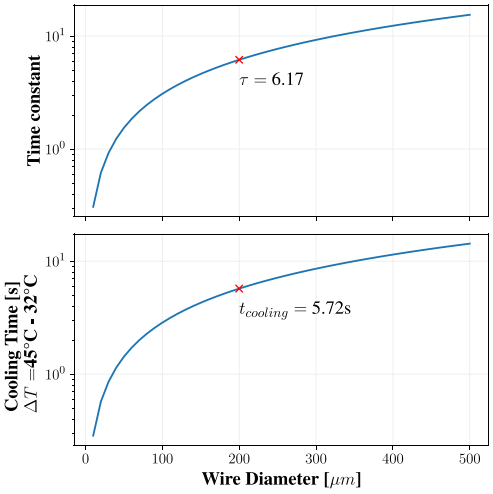

Fig. 5. Extrapolation of the cooling time based on wire diameter with H = 43.8 $Wm^{-2}K^{-1}$ [20].

torsional stress, the actuator can be estimated to last around 10^3 – 10^5 cycles before failure.

4. Inchworm implementation

The proof of concept SMA mechanical oscillator presented in Section 3, is adapted to create a crawling robot that mimics the locomotion of an inchworm. Due to the purely mechanical nature of the oscillator design, the robot can be made to crawl across a surface without the presence of a micro-controller or other control logic.

4.1. Working principle

The basic working principle of the inchworm robot consists of transforming the linear movement of the SMA oscillator into a rotation of a pair of legs such that the tips (or claws) of the robot leg pulls the body of the robot across the ground.

As seen in Fig. 6, the inchworm robot is entirely 3D printed in a single piece and is powered using an SMA coil. The oscillator system is implemented using a magnetic latch system as presented in Section 3. The insect legs are attached to the free end of the SMA coil so as to harness the strain recovery when the coil is heated. Here, the flexural linear stage is replaced with simple cantilever leaf springs so as to transform the linear contraction of the SMA coil into a rotation of the insect legs.

The robot functions in a similar manner to the inchworm presented in Section 2.1 where the legs alternate between high friction and low friction with respect to the ground allowing the robot to crawl. Here, the alternating friction of the legs is made possible by

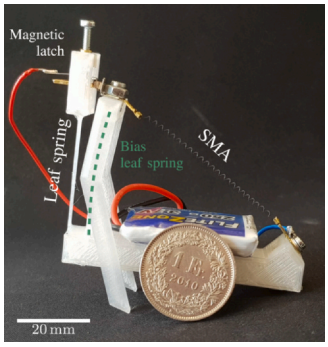

Fig. 6. The implementation of the insect robot around the mechanical SMA oscillator.

the design of the tips of the insect legs. The tips or claw of the insect robot legs is designed such that the angle of contact with the ground surface is asymmetrical with the direction of movement. It behaves in a similar way to a ratchet system where one degree of freedom is allowed in the forward direction but not in the backward direction. This claw design allows the insect leg to rotate forward in the clockwise direction but prevents any rotation in the anti-clockwise direction due to changes in friction with respect to the ground. As the SMA coil is stretched by the bias leaf spring during cooling, the entire insect body is dragged forward by the insect legs due to its rotation being blocked in the backward direction. Thus, to summarize, during the heating of the SMA coil, the legs advance forward and during the cooling of the SMA coil, the entire body of the insect robot advances forward to return the structure to its original state.

4.2. Analytical model

An analytical model can help with sizing the body of the insect robot so as to determine the expected displacement of the insect robot based on the contraction of the SMA coil.

As mentioned, in Section 4.1, the crux of the design revolves around the cantilever leaf spring. This flexural structure converts the linear contract of the SMA coil into the rotation of the insect legs while also serving as the bias spring for SMA actuator allowing the coil to be stretched during the cooling phase.

The pseudo-rigid-body model [17] is used to model flexure-based mechanisms such as the cantilever beam as traditional rigid-body mechanisms. Thus, by simplifying the cantilever leaf spring as a virtual pivot, an analytical model can be established to estimate the effect of the SMA coil contraction. In the work [22], the location of the virtual pivot can be estimated with relative accuracy to a point at a distance of aL from the clamped end of the cantilever beam, where L is the length of the beam, bL is the length of the rigid attachment point with the SMA coil and a is:

$$a = \frac{1 + 3b}{3 + 6b} \tag{6}$$

The pre-stretched SMA coil of length, L'_{SMA}, is attached to the biasing cantilever leaf spring at the free end as shown in Fig. 7. The position of cantilever tip, $P(x_P, y_P)$, as the SMA coil contracts in length by ε, can be deduced by finding the intersection between the two circles with radii, r_1 and r_2, and with centres at the virtual pivot V (x_V, y_V) and fixed end of the SMA coil $S(x_S, y_S)$, respectively.

$$P(x, y) = \frac{1}{2}\begin{pmatrix} x_V + x_S \\ y_V + y_S \end{pmatrix} + \frac{r_1^2 - r_2^2}{2R^2}\begin{pmatrix} x_S - x_V \\ y_S - y_V \end{pmatrix} \pm \frac{1}{2}\sqrt{2\frac{r_1^2 + r_2^2}{R^2} - \frac{(r_1^2 - r_2^2)^2}{R^4} - 1}\begin{pmatrix} y_S - y_V \\ x_V - x_S \end{pmatrix} \tag{7}$$

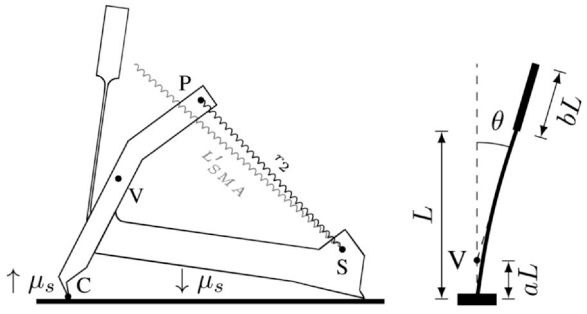

Fig. 7. The working principle of the insect robot showing the simplification of the cantilever beam to a virtual rigid body pivot. The claw design changes the coefficient of friction (μ_s) of the insect with respect to the ground allowing the robot to crawl.

where R is the Euclidian distance, $|\overline{VS}|$, between the two circle centres, $r_1 = (1 - a + b)L$ and $r_2 = L'_{SMA} - \varepsilon$ representing the current length of the SMA coil.

As the insect legs are attached at the cantilever tip, the claw tips, $C(x_C, y_C)$, of the insect robot can be estimated by using a series of simple translation and rotation transformations from the cantilever tip based on the angles (α) and lengths (L) of the insect leg segments.

$$C(x, y) = \begin{pmatrix} x_P \\ y_P \end{pmatrix} + \sum_{i=1} L_i \begin{pmatrix} \cos(-\frac{\pi}{2} - \theta + \sum_{i=1} \alpha_i) \\ \sin(-\frac{\pi}{2} - \theta + \sum_{i=1} \alpha_i) \end{pmatrix} \tag{8}$$

Thus, based on the contraction of the SMA coil (ε), the step length of the insect, ΔC, can be estimated by taking the Euclidean distance between the claw tip location before and after the SMA contraction. The position of the insect robot claw and the step length based on the SMA coil contraction can be seen in Fig. 9.

5. Results and discussion

5.1. Oscillator prototype

The proof of concept oscillator prototype, as described in Section 3, was 3D printed using PLA filament and was supplied with a constant current and left to oscillate for 2 min. By measuring the temperature fluctuations with a thermal camera, the frequency and periodicity were measured, as shown in Fig. 8. The rise time and cooling times were measured by detecting the peaks and troughs of the signal. The mean and standard deviation of these values were then calculated. The rise time of the oscillator when supplied with 340 mA was measured to be 3.8 ± 0.18 s while the rise time when supplied with 840 mA was measured to be 0.64 ± 0.09 s. The cooling time when supplied with 340 mA and 840 mA was found to be 5.71 ± 0.09 s and 5.82 ± 0.2 s, respectively. Thus, the period of the oscillations for the two measurements was found to be 9.60 ± 0.17 s and 6.47 ± 0.22 s which corresponds to a frequency of 0.10 Hz and 0.16 Hz, respectively. The cooling time predicted based on the SMA geometry, as shown in Fig. 5, corresponds to the measured values. Also, the cooling time remains relatively constant with respect to the varying current across the SMA. These results show that this oscillator design using the magnetic latch system can be used to create an inchworm robot with a constant speed and that can be sized for a certain speed.

The oscillator prototype showed that the electrical contact established with the magnet was less than ideal. Large spikes in current was observed as the SMA made contact with the magnet. In the case of the inchworm robot, the electrical contact was adapted to use contacts salvaged from an electrical relay. This improved considerably the current flow and allowed for a more constant oscillating frequency.

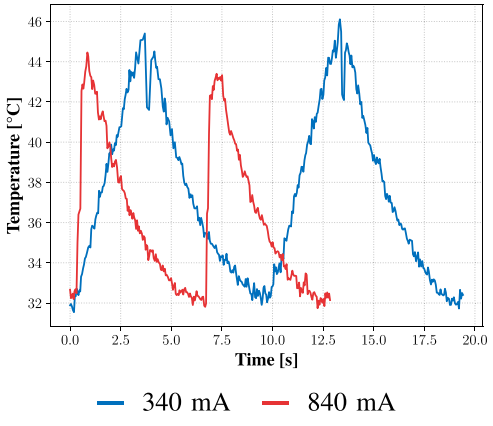

Fig. 8. Effect of the current on the evolution of the SMA spring's temperature on the oscillator. The temperature of the SMA coil was measured using a thermal camera with an optical zoom lens that allows for high spatial resolution.

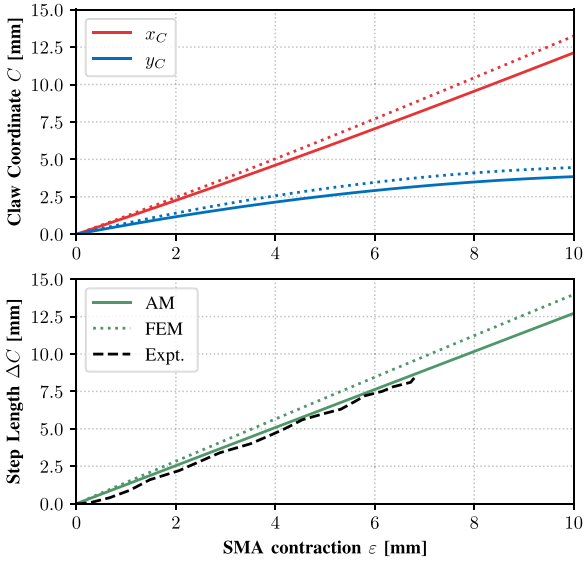

Fig. 9. Comparison of the leg tip displacement versus the contraction of the SMA coil between the analytical model (AM) and Finite Element Model (FEM) simulation. Here, the dotted and filled lines represent the FEM results and analytical model, respectively.

5.2. Inchworm robot

The analytical model of the inchworm robot was used to predict the step length based on the contraction of the SMA coil during heating. The validation of this analytical model was performed by simulating the entire robot using a commercial finite element modelling (FEM) software and comparing it with the results of the analytical model, as shown in Fig. 9. The model is further validated by the experimental results of the inchworm prototype, as shown in the same figure. The comparison shows that the analytical model is quite accurate and can be an ideal candidate for the optimization of the step length.Fig. 10.

The inchworm robot was fabricated using a single 3D printed piece from PLA filament based on the parameters shown in Table 1, as seen in Fig. 6 and Fig. 7. By connecting the robot to a 3.7 V 20 mAh battery (LP201515), the robot is able to crawl untethered, as shown in Fig. 11, for an estimated 1.6 min. The total weight of the robot including the battery weighs 9.7 g. When left to crawl on a flat surface, an average speed of 1.55 mms^{-1} was measured, as shown in Fig. 10. The efficiency of the robot legs is highly dependant on the

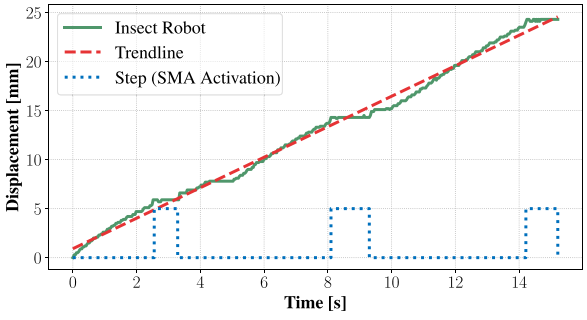

Fig. 10. The displacement of the insect robot. The average speed of the robot is 1.55 mms^{-1}. Here, the step line represents the state of the SMA. A high value denotes that the SMA coil is being heated and a low state denotes that the SMA coil is cooling down.

Table 1
The design parameters of the inchworm robot.

Parameter	Value
SMA dimensions	Coil: ⌀1.37 × 12 mm Wire: ⌀0.2 mm
Biasing Leaf Spring	30 × 10 × 0.6 mm
Magnet Leaf Spring	30 × 2.5 × 0.6 mm
Magnet force	250 g
Battery Life	1.6 min @ 20 mAh
Leg dimensions	L_i = [20 mm, 33.5 mm]α_i = [0°, 26.6°]

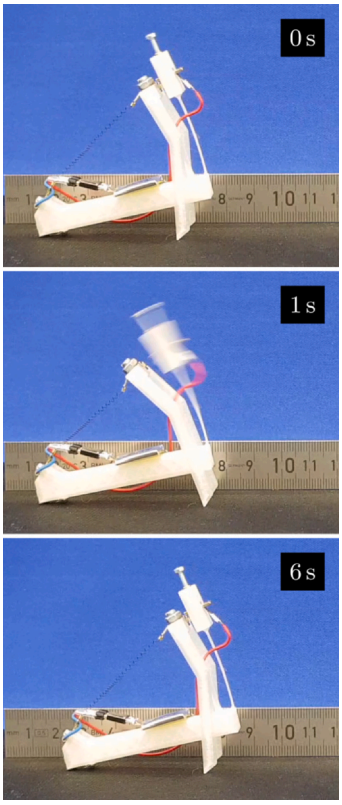

Fig. 11. The untethered gait of the insect robot with a step length of 8.4 mm.

surface; smoother surfaces cause the legs to slip and drastically changes the efficiency of the design.

The insect robot is powered using a single 200μm diameter SMA coil, provided by *Dynalloy*. The coil is heating using Joule's heating by passing a current through it with the help of a small battery. The heating consists of passing a current of 770 mA for around 750 ms with a power of 1.7 W. The robot was measured to have a step size of 8 mm. Often, in the case of inchworm robots, the cost of transport (CoT) is calculated to compare the different implementations. This indicator allows for the comparison of dissimilar animals and modes of transportation. It can be calculated using the following equation, $\text{CoT} = E/mgd$, where E is the energy required to heat the SMA, m is the total mass of the robot including the battery, g is the acceleration due to gravity and d is the step length of the robot. Using the equation, the CoT was calculated to be around 1620 $\text{Jkg}^{-1}\text{m}^{-1}$. This is comparable to other untethered inchworm robots like in the work by [23] whose CoT is measured to be 1670 $\text{Jkg}^{-1}\text{m}^{-1}$.

When compared to other inchworm robots, as shown in Fig. 12, this work is able to achieve comparable speeds to similar tethered alternatives and is extremely lightweight due to the absence of any sensors or electronics. This work is however limited by its dependence on passive cooling. The design, while being cheap and easily fabricated using 3D printing, it is limited by the PLA material. By optimizing the material to create thinner leaf springs, the size of the

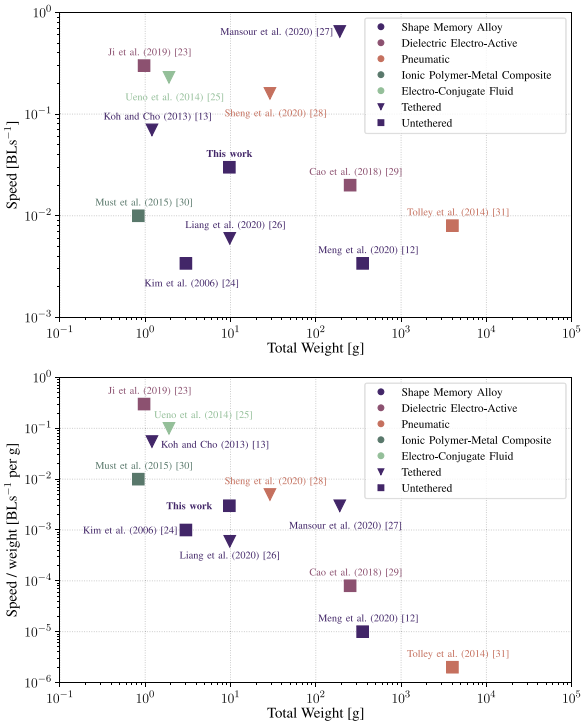

Fig. 12. The distribution of various different inchworm robots powered by smart materials based on their total weight, speed and speed / weight ratio (in Body Lengths (BL) per second and in Body Lengths (BL) per second per gram, respectively) [24–31].

robot can be greatly reduced. Future work will have to include the optimization of the claw design and improve the overall efficiency of the insect robot's claw design to prevent slipping.

6. Conclusion

This work presents a 3D printed crawling inchworm robot powered by an SMA powered mechanical oscillator actuated. This novel oscillator is actuated using a single SMA coil without the need for any control strategy or electronics. The system uses flexure-based mechanisms to create a magnetic latch system that is the crux of the system. A flexural cantilever beam is further used as a biasing element for the SMA actuator while also acting as the motion conversion system that transmits the linear contraction of the SMA coil to the movement of the robot legs. This concept of using the inherent stiffness of a flexure-based mechanism could be widely used in other applications to create SMA actuators that are lightweight, compact and easy to assemble. The SMA insect robot weighs only 9.7 g and has an average speed of 1.55 mms^{-1}.

A thermal model for the cooling of the SMA is presented and validated. An extrapolation of this model for varying SMA wire diameters is presented so as to easily size the required speed of the robot. An analytical model of the step length of the inchworm robot is presented and further validated using a FEM simulation.

In this work, an innovative approach to designing SMA-based actuators combined with flexural systems is presented. A system in which, such an actuator can be harness as a mechanical oscillator without the need for any electronics is exploited to create a mobile crawling robot. This system, being lightweight and easy to manufacture, can be integrated into larger robots with multiple crawling legs.

For future work, the leg design needs to be optimized to increase the step length of the robot. Furthermore, the current implementation of the claw design is inefficient and will require further investigation to improve the efficiency of the crawling gait.

CRediT authorship contribution statement

Sean Thomas Conceptualization, Methodology, Validation, Investigation, Visualization, Writing - original draft preparation; **Paolo Germano** Conceptualization; **Thomas Martinez** Review & editing, Validation; **Yves Perriard** Supervision, Project administration, Validation.

Declaration of Competing Interest

The authors declare that they have no known competing financial interests or personal relationships that could have appeared to influence the work reported in this paper.

Appendix A. Supporting information

Supplementary data associated with this article can be found in the online version at doi:10.1016/j.sna.2021.113115.

References

[1] J. Mohd Jani, M. Leary, A. Subic, M.A. Gibson, A review of shape memory alloy research, applications and opportunities, Mater. Des. (1980-2015) 56 (. 2014) 10780–11113.

[2] A. Nespoli, S. Besseghini, S. Pittaccio, E. Villa, S. Viscuso, The high potential of shape memory alloys in developing miniature mechanical devices: a review on shape memory alloy mini-actuators, Sens. Actuators A: Phys. 158 (. 2010) 149–160.

[3] P. Motzki, F. Khelfa, L. Zimmer, M. Schmidt, S. Seelecke, Design and validation of a reconfigurable robotic end-effector based on shape memory alloys, IEEE/ASME Trans. Mechatron. (2019).

[4] H., Rodrigue, W., Wang, M.-W., Han, T.J., Kim, S.-H., Ahn, An Overview of Shape Memory Alloy-Coupled Actuators and Robots, Soft Robotics 4 (1) Feb. 20173–15. Publisher: Mary Ann Liebert, Inc., publishers.

[5] D. Lagoudas, L. Machado, M. Lagoudas, Nonlinear vibration of a one-degree of freedom shape memory alloy oscillator: a numerical-experimental investigation, 46th AIAA/ASME/ASCE/AHS/ASC Structures, Structural Dynamics and Materials Conference, American Institute of Aeronautics and Astronautics,, Austin, Texas, 2005.

[6] T., Sakagami, K., Seki, M., Iwasaki, Sensorless Position Control Based on Resistance and Heat Transfer Models in Shape Memory Alloy Actuators, in: 2019 IEEE/ASME International Conference on Advanced Intelligent Mechatronics (AIM), Jul. 2019, pp. 217–222. ISSN: 2159–6255.

[7] N.A., Mansour, Y., Kim, ANFIS-Based System Identification and Control of a Compliant Shape Memory Alloy (SMA) Rotating Actuator, in: IEEE Robotics & Automation Magazine, volume 16, Boston, MA, Jul. 2020, pp. 81–94.

[8] P. Narayanan, M. Elahinia, Control of a shape memory alloy–actuated rotary manipulator using an artificial neural network–based self-sensing technique, J. Intell. Mater. Syst. Struct. 27 (2016) 1885–1894.

[9] M.-S. Kim, W.-S. Chu, J.-H. Lee, Y.-M. Kim, S.-H. Ahn, Manufacturing of inchworm robot using shape memory alloy (SMA) embedded composite structure, Int. J. Precis. Eng. Manuf. 12 (2011) 565–568.

[10] M.M. Kheirikhah, S. Rabiee, M.E. Edalat, A review of shape memory alloy actuators in robotics, in: J. Ruiz-del Solar, E. Chown, P.G. Plöger (Eds.), RoboCup 2010: Robot Soccer World Cup XIV, Springer, Berlin, Heidelberg, 2011, pp. 206–217.

[11] Y.P., Lee, B., Kim, M.G., Lee, J.-O., Park, Locomotive mechanism design and fabrication of biomimetic micro robot using shape memory alloy, in: IEEE International Conference on Robotics and Automation, 2004. Proceedings. ICRA '04. 2004, volume 5, Apr. 2004, pp. 5007–5012 Vol.5.

[12] L. Meng, R. Kang, D. Gan, G. Chen, L. Chen, D.T. Branson, J.S. Dai, A mechanically intelligent crawling robot driven by shape memory alloy and compliant bistable mechanism, J. Mech. Robot. 12 (2020).

[13] J.-S. Koh, K.-J. Cho, Omega-shaped inchworm-inspired crawling robot with large-index-and-pitch (LIP) SMA spring actuators, IEEE/ASME Trans. Mechatron. 18 (2013) 419–429.

[14] C., Liang, Y., Wang, T., Yao, B., Zhu, A shape memory alloy–actuated soft crawling robot based on adaptive differential friction and enhanced antagonistic configuration. J. Intell. Mater. Syst. Struct. 31 (16) Sep. 20201920–1934. Publisher: SAGE Publications Ltd STM.

[15] W., Wang, J.-Y., Lee, H., Rodrigue, S.-H., Song, W.-S., Chu, S.-H., Ahn, Locomotion of inchworm-inspired robot made of smart soft composite (SSC), Bioinspiration & Biomimetics 9 (4) Oct. 2014046006. Publisher: IOP Publishing.

[16] F., Cosandier, S., Henein, M., Richard, L., Rubbert, The art of flexure mechanism design2017. [Online]. Available: ⟨http://infoscience.epfl.ch/record/232450⟩.

[17] L. L. Howell, S. P. Magleby, B. M. Olsen (Eds.), Handbook of Compliant Mechanisms, John Wiley & Sons, Inc, Chichester, West Sussex, United Kingdom; Hoboken, 2013.

[18] S. Thomas, M. Almanza, Y. Perriard, Design analysis of a shape memory alloy bias-spring linear actuator, 2019 12th Int. Symp. . Linear Drives Ind. Appl. (LDIA) (2019) 1–5.

[19] L. Brinson, One-dimensional constitutive behavior of shape memory alloys: thermomechanical derivation with non-constant material functions and redefined martensite internal variable, J. Intell. Mater. Syst. Struct. 4 (1993) 229–242.

[20] S., Thomas, P., Germano, T., Martinez, Y., Perriard, Control-Free Mechanical Oscillator Powered by Shape Memory Alloys, in: 2021 IEEE/ASME International Conference on Advanced Intelligent Mechatronics (AIM), Delft, The Netherlands, 2021, p. 5.

[21] A. Runciman, D. Xu, A.R. Pelton, R.O. Ritchie, An equivalent strain/Coffin–Manson approach to multiaxial fatigue and life prediction in superelastic Nitinol medical devices, Biomaterials 32 (22) (2011) 4987–4993. Aug.

[22] X.M., Zhang, A.Q., Liu, C., Lu, D.Y., Tang, A real pivot structure for MEMS tunable lasers. J. Microelectromech. Syst. 16 (2) Apr. 2007269–278. Conference Name: Journal of Microelectromechanical Systems.

[23] X. Ji, X. Liu, V. Cacucciolo, M. Imboden, Y. Civet, A. El Haitami, S. Cantin, Y. Perriard, H. Shea, An autonomous untethered fast soft robotic insect driven by low-voltage dielectric elastomer actuators, Sci. Robot. 4 (2019) eaaz6451.

[24] B. Kim, M.G. Lee, Y.P. Lee, Y. Kim, G. Lee, An earthworm-like micro robot using shape memory alloy actuator, Sens. Actuators A: Phys. 125 (2) (2006) 429–437.

[25] S. Ueno, K. Takemura, S. Yokota, K. Edamura, Micro inchworm robot using electro-conjugate fluid, Sens. Actuators A: Phys. 216 (2014) 36–42.

[26] C. Liang, Y. Wang, T. Yao, B. Zhu, A shape memory alloy-actuated soft crawling robot based on adaptive differential friction and enhanced antagonistic configuration, J. Intell. Mater. Syst. Struct. 31 (16) (2020) 1920–1934 (publisher: SAGE Publications Ltd STM).

[27] N.A. Mansour, T. Jang, H. Baek, B. Shin, B. Ryu, Y. Kim, Compliant closed-chain rolling robot using modular unidirectional SMA actuators, Sens. Actuators A: Phys. 310 (2020) 112024.

[28] X. Sheng, H. Xu, N. Zhang, N. Ding, X. Zhu, G. Gu, Multi-material 3D printing of caterpillar-inspired soft crawling robots with the pneumatically bellow-type body and anisotropic friction feet, Sens. Actuators A: Phys. 316 (2020) 112398.

[29] J. Cao, L. Qin, J. Liu, Q. Ren, C.C. Foo, H. Wang, H.P. Lee, J. Zhu, Untethered soft robot capable of stable locomotion using soft electrostatic actuators, Extrem. Mech. Lett. 21 (2018) 9–16.

[30] I. Must, F. Kaasik, I. Põldsalu, L. Mihkels, U. Johanson, A. Punning, A. Aabloo, Ionic and capacitive artificial muscle for biomimetic soft robotics, Adv. Eng. Mater. 17 (1) (2015) 84–94.

[31] M.T. Tolley, R.F. Shepherd, B. Mosadegh, K.C. Galloway, M. Wehner, M. Karpelson, R.J. Wood, and G.M. Whitesides, A Resilient, Untethered Soft Robot, Soft Robotics, 1, 3, 213–223, Aug. 2014, publisher: Mary Ann Liebert, Inc., Publishers.

Sean Thomas was born in Vellore, India, in 1992. He received the M.Sc. degree in micro-engineering with a specialization in robotics, from the Swiss Federal Institute of Technology (EPFL), Lausanne, Switzerland, in 2017. He is currently working toward the Ph.D. degree with the Integrated Actuator Laboratory, EPFL. His research interests are in the field of shape memory alloys, control systems, and mechanical design.

Paolo Germano was born in Lausanne, Switzerland, in 1966 and is native of Italy and Switzerland. He received the M.Sc. in micro-engineering from the Swiss Federal Institute of Technology (EPFL) Lausanne in 1990. He is currently a senior researcher at the Integrated Actuators Laboratory. His activities as project leader are mainly focused on test benches dedicated to different types of actuators. In the domain of contactless power transmission, he took part in projects in the biomedical field, in the field of electrical vehicles as well as various projects related to machine tools and wireless computer peripheral supplies.

Thomas Martinez received the Engineering degree in electrical engineering from Ecole Polytechnique, Palaiseau, France, in 2015, and the M.Sc. degree in micro- and nano-electronics from the Swiss Federal Institute of Technology (EPFL), Lausanne, Switzerland, in 2016. He received his Ph.D. in Electrical Engineering in 2019 from University Paris-Saclay. He currently works as a postdoctoral researcher in the Integrated Actuators Laboratory in the Swiss Federal Institute of Technology. His research interests include piezoelectric devices for energy conversion, low-power electronics, dielectric elastomer and SMA actuators.

Yves Perriard received the M.Sc. and Ph.D. degrees in microengineering from the Swiss Federal Institute of Technology (EPFL), Lausanne, in 1989 and 1992, respectively. He was the co-founder and Chief Executive Officer of Micro-Beam SA involved in high-precision electric drives. He is with EPFL, Neuchatel, Switzerland, where he was a Senior Lecturer in 1998, has been a Professor since 2003, and is currently the Director of the Integrated Actuators Laboratory.